

Supplemental Figure Legends:

Figure S1, related to Figure 1: Food consumption and serum biomarker results. (A)

Cumulative food consumption (kcal/mouse \pm SEM, n=24) and (B) individual calories consumed (kcal/mouse/week \pm SEM, n=24). As in previous experiments (see ref 11), there is no difference between FT and NA mice. Serum quantification (\pm SEM) of (C) alanine transaminase (ALT) activity and (D) triglycerides in overnight fasted mice (n=6 per groups; measures were repeated twice independently).

Figure S2, related to Figure 2: Gut microbiome dynamics. (A) Heatmap of cycling OTUs

organized by peak from NA mice. Corresponding heatmap of the OTUs from other conditions are shown to illustrate that phases and cycling changed with diet and TRF. Bar graph at the bottom of column shows the time point at which the OTUs peaked. Black and white boxes show light on/light off timing. Yellow box shows when mice had access to food. (B) Log₂ plot of percent reads of OTUs that are found in all three feeding conditions. The x-axis is log₂ of the average (across all time points, n=18) of percent reads of an OTU in NA divided by its percent reads in FA. When positive, this would indicate that a particular OTU is more common in NA than in FA, and when negative, that it is less common in NA compared to FA. Likewise, the y-axis is the log₂ of the average (across all time points, n=18) of percent reads of an OTU in FT divided by its percent reads in FA. When positive this would indicate that a particular OTU is more common in FT than in FA, and when negative, that a particular OTU is less common in FT compared to FA. This panel shows OTUs that are non-cycling and those that are cycling in NA. OTUs that cycled in NA were much more common in the NA gut microbiome than they were in FA gut microbiome (p < 0.0005, Chi-square test). (C) Is a similar log₂ plot as (B) but shows all OTUs that were common to all three feeding conditions. (D) Venn diagrams showing the number of total OTUs that were shared

between the three feeding conditions and (E) the number of cycling OTUs that were shared between the three feeding conditions. Heatmap of cycling OTUs organized by peak from (F) FA mice and (G) FT mice. Corresponding heatmap of the OTUs from other conditions are shown to illustrate that phases and cycling changed with diet and TRF. Bar graph at the bottom of column shows the time point at which the OTUs peaked. Black and white boxes show light on/light off timing. Yellow box shows when mice had access to food. Diurnal activity of the phylum Actinobacteria (H) and Proteobacteria (I). First column: double plot of percent read for a particular genus from all three conditions (n=3/condition/time point). Second column: double plot of percent reads for the genus from the two HFD conditions (n=3/condition/time point). Third column: histogram of percent total reads that this genus comprises in each condition (n=18/condition). Fourth column: histogram showing percent reads that are expressed when light off/light on (n=9). Fifth column: histogram showing percent reads that are expressed when food from nighttime feeding has reached the cecum (ZT 17, 21, 1) and during relative fasting (ZT 5, 9, 13; n=9, see Figure 1 and ref 20). * p < 0.05.

Figure S3, related to Figure 3: Subphylum analysis of the gut microbiome. Diurnal activity of genera identified in our study. First column: double plot of percent read (\pm SEM, n=3 per time point) for a particular genus from all three conditions. Second column: double plot of percent reads (\pm SEM, n=3 per time point) for the genus from the two HFD conditions. Third column: histogram of percent total reads (\pm SEM, n=18) that this genus comprises in each condition. Fourth column: histogram showing percent reads (\pm SEM, n=9) that are expressed when light off/light on. Fifth column: histogram showing percent reads (\pm SEM, n=9) that are expressed when food from nighttime feeding has reached the cecum (ZT 17, 21, 1) and during relative fasting (ZT 5, 9, 13; see Figure 1 and ref 20). * p < 0.05.

Figure S4, related to Figure 4: TRF restores cyclical fluctuation in genera thought to be involved in metabolism. (A) Percent reads (\pm SEM, n=3 per time point) of a double plot of genus *Oscillibacter* from all three conditions. (B) Genera based principle component analysis (PCA) of FA and FT mice. Green vectors show the axis where that particular genus accounted for most of the variability.

Figure S5, related to Figure 5: Diversity analysis. (A) Rarefaction curve of average reads from specific time points in FA and FT (number in box is ZT time point) (n=3/condition). The rarefaction plots of FT mice at ZT 9 and 21 were remarkably different, whereas those from FA mice at ZT 9 and 21 were quite similar. (B) Triangle plots illustrating β -diversity (see Koleff et al., 2003 and **Fig 3F, 3G**). Briefly, points that are close to apex (a') share many OTUs. However points that are near the base (b' or c') have many dissimilarities. These plots show that NAVFA and NAVFT have the most dissimilarities and are nearly indistinguishable. NAVNA have much more dissimilarity than the FAVFA and FTvFT.

Figure S6, related to Figure 6: Metabolites that are processed by gut microbes are differentially excreted in the feces of mice in different conditions. (A) Average relative quantification of xylose and galactose (\pm SEM) in the feces (n = 4 samples from each condition, from separate cages) which includes results from all three conditions. Absolute quantification in pmol/mg of feces of the primary bile acids MCA, CA and DCA, the secondary bile acids DCA, UDCA and LCA and their respective tauro (T-) and glyco (G-) conjugates. CA: Cholate, CDCA: Chenodeoxycholate, MCA: Muricholate (a: alpha-, b: beta-, g: gamma-, w:omega-), DCA: Deoxycholate, UDCA: ursodeoxycholate, LCA: lithocholate, T-: Tauro-, G-:Glyco.

Figure S1

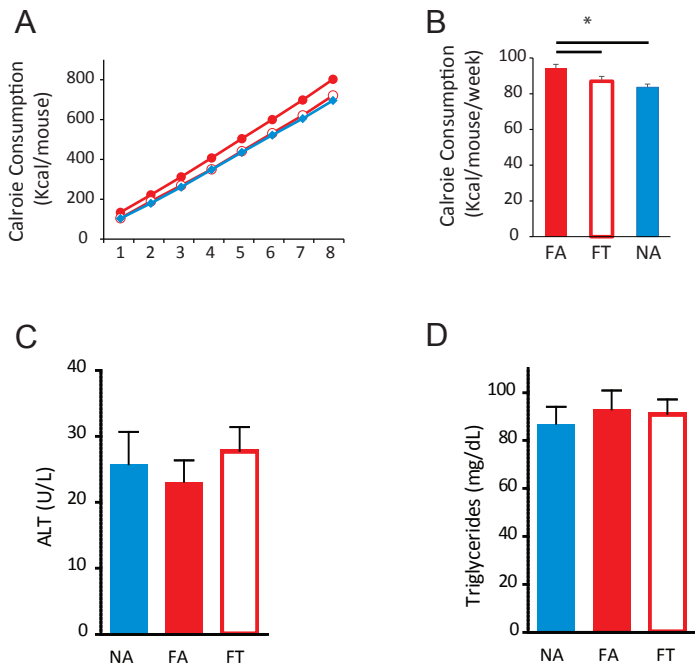


Figure S2

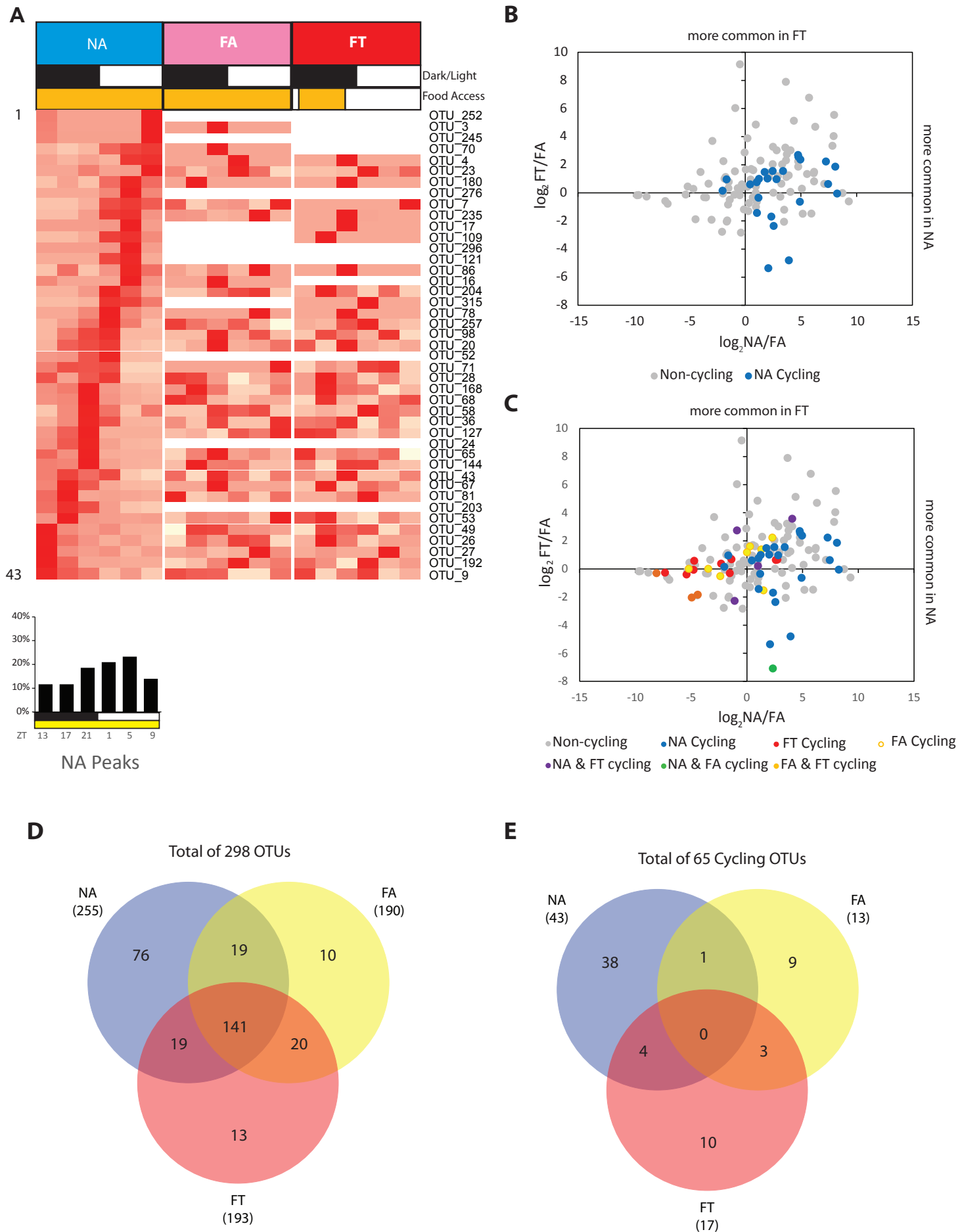


Figure S2 (cont.)

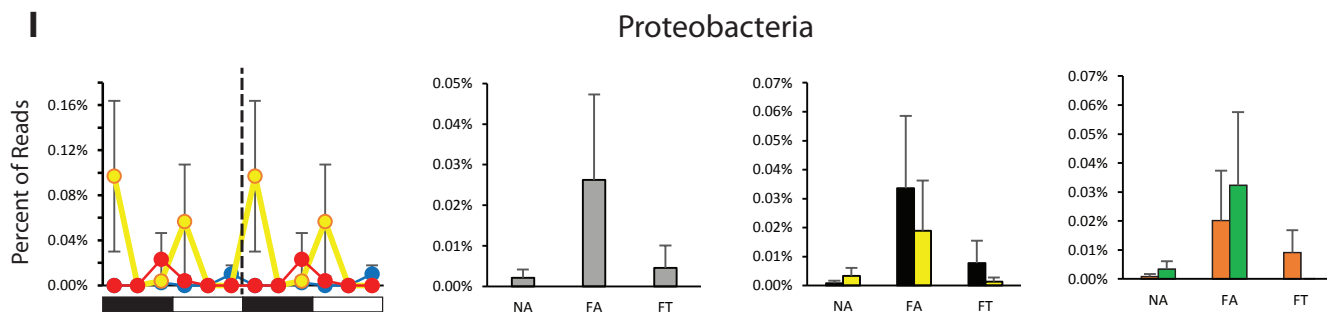
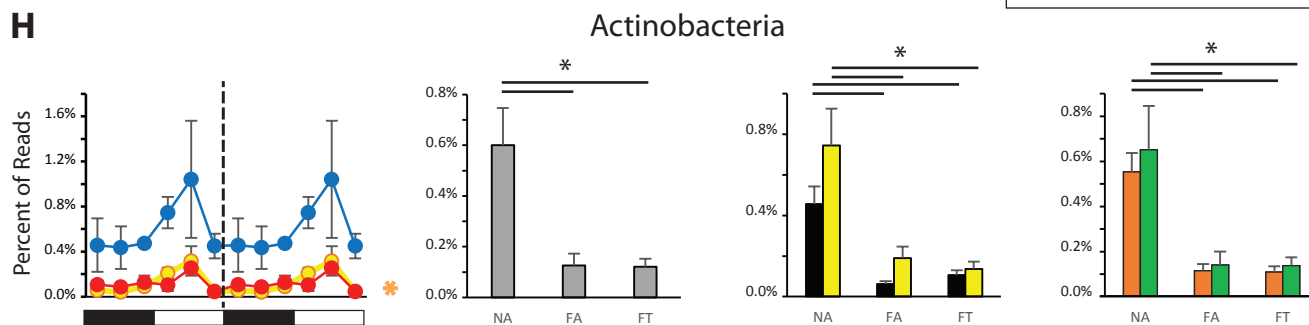
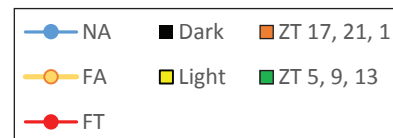
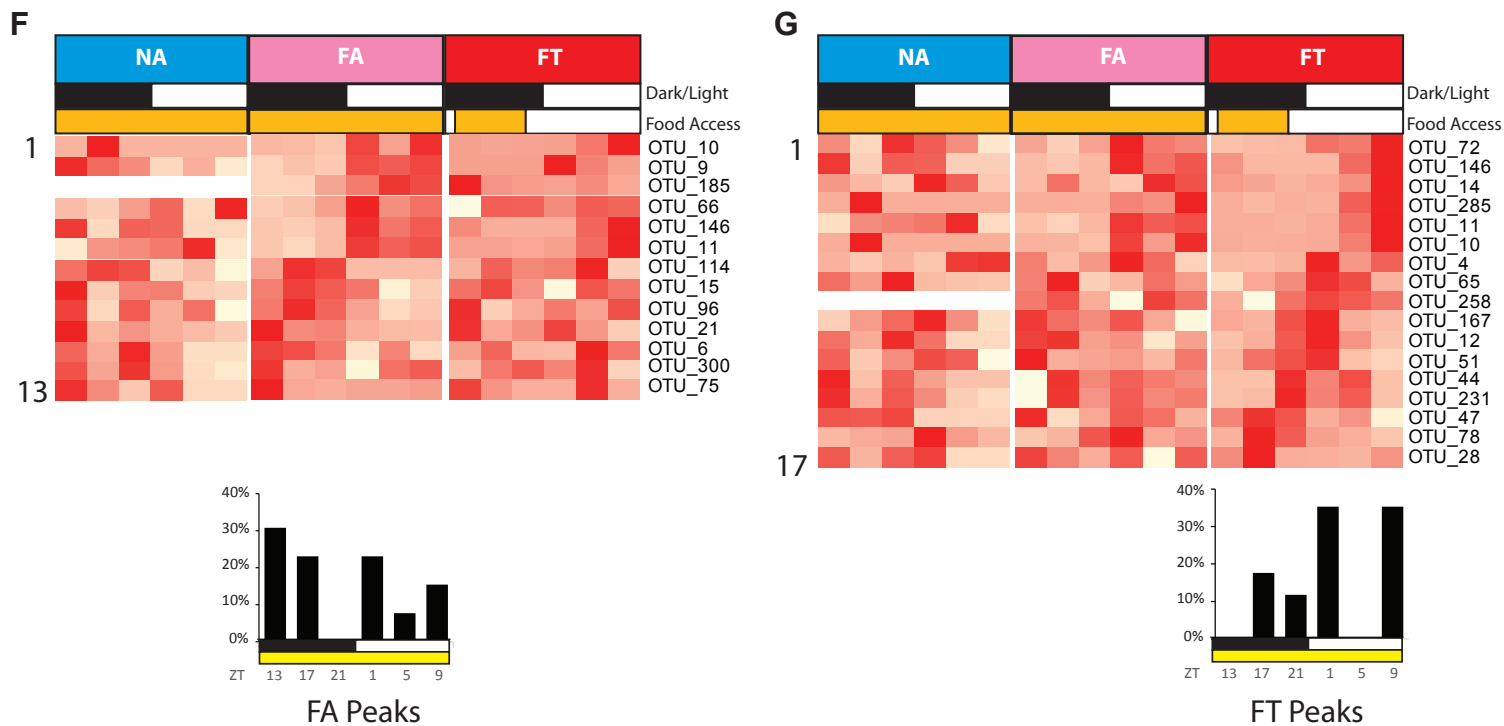


Figure S3

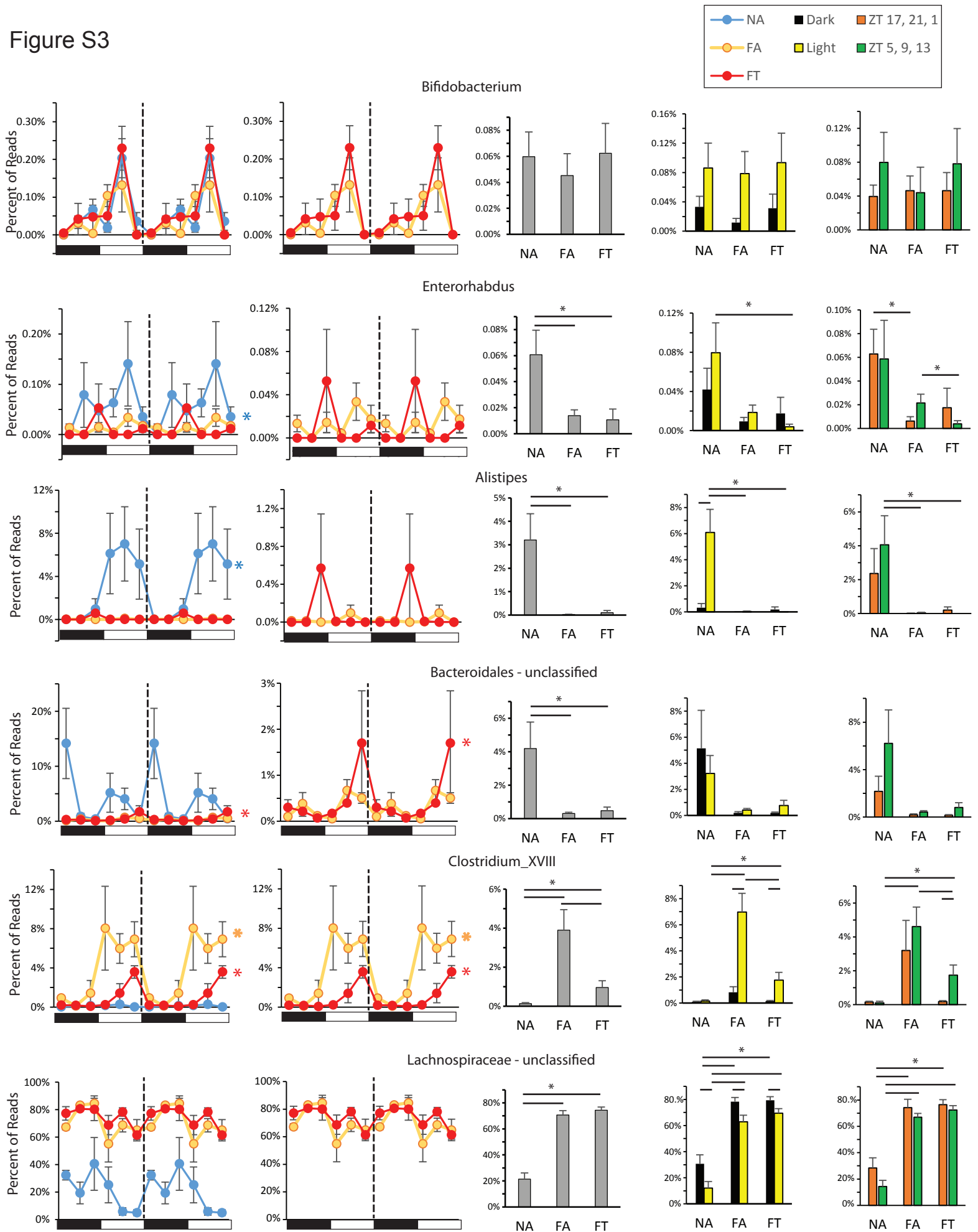
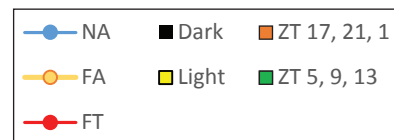
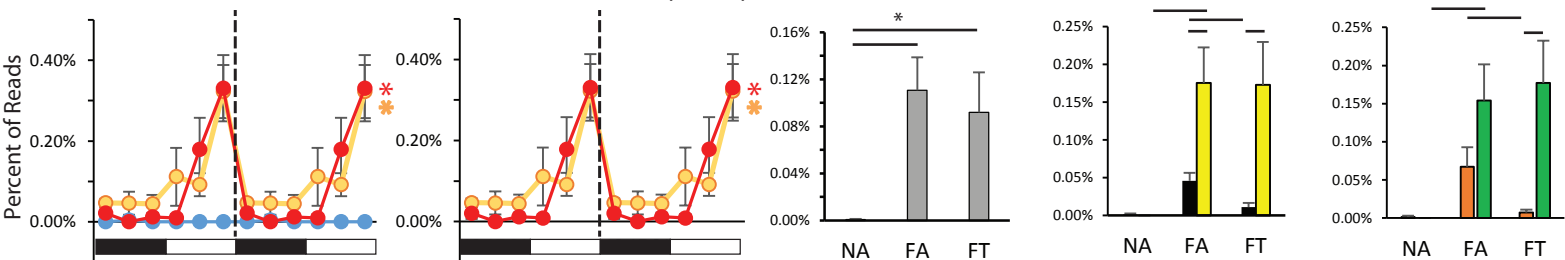


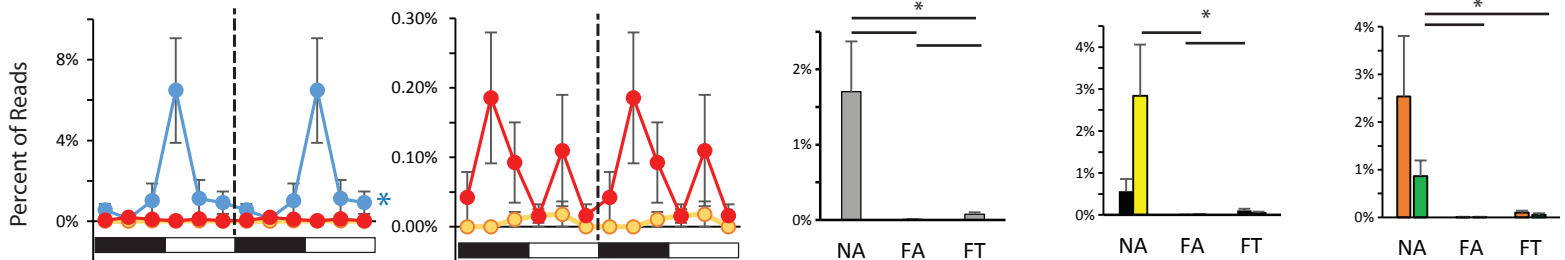
Figure S3 (cont.)



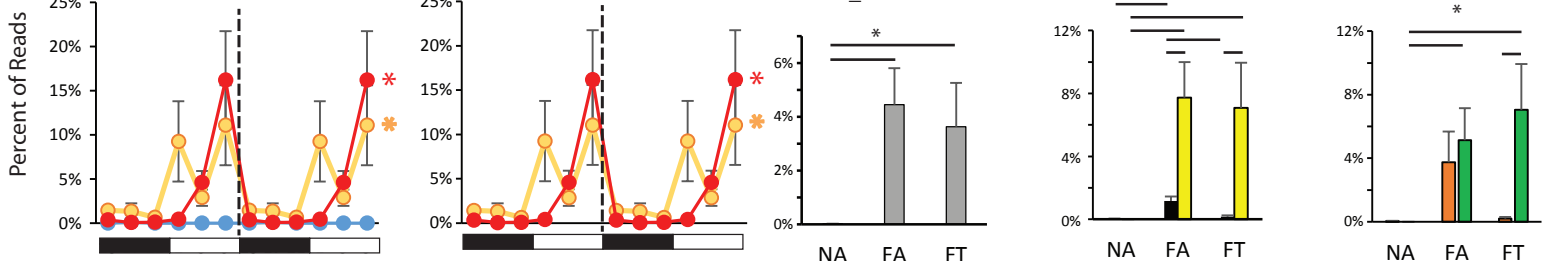
Peptostreptococcaceae - unclassified



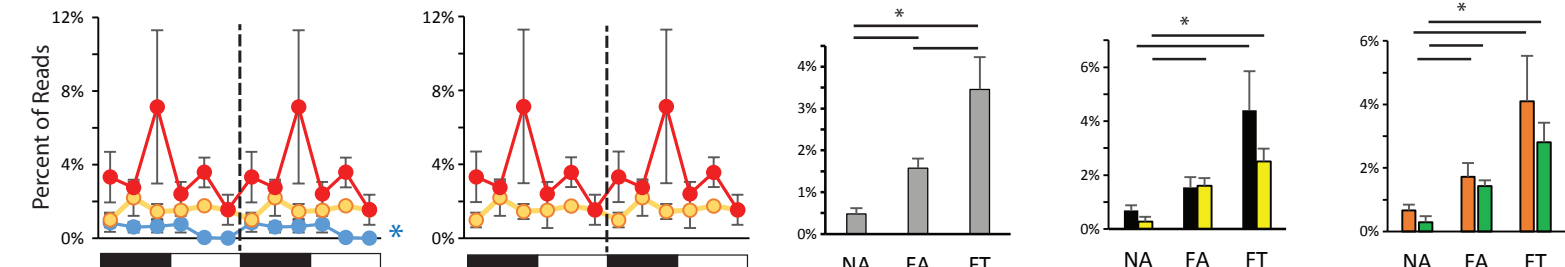
Blautia



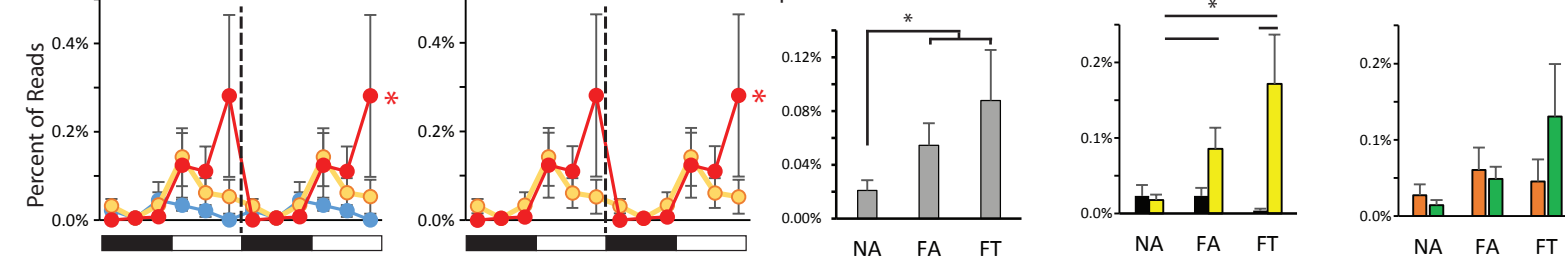
Clostridium_XI



Pseudoflavonifractor



Coprobacillus



Akkermansia

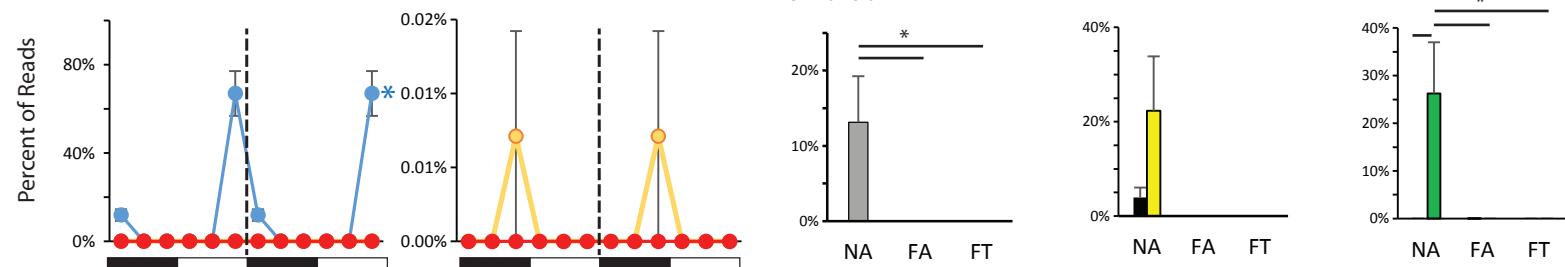


Figure S4

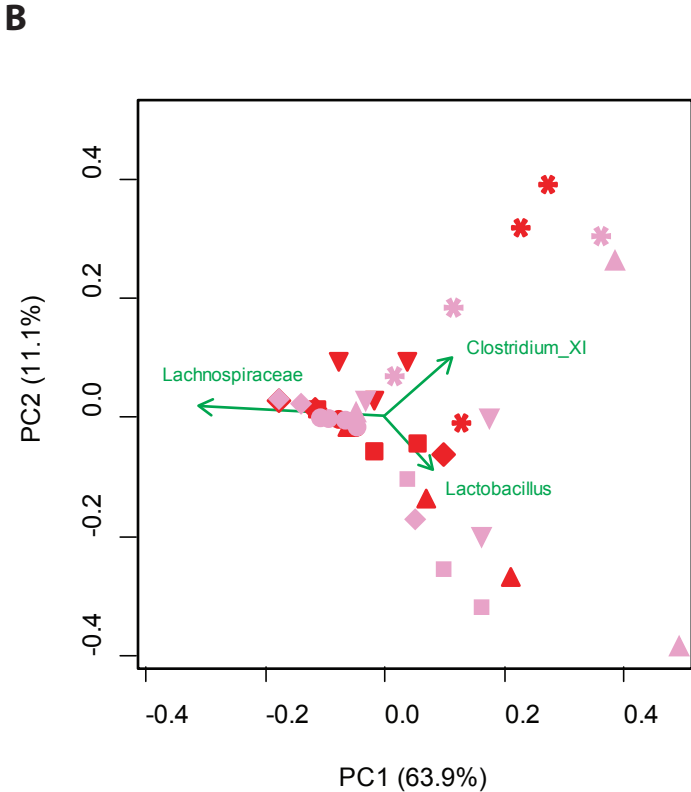
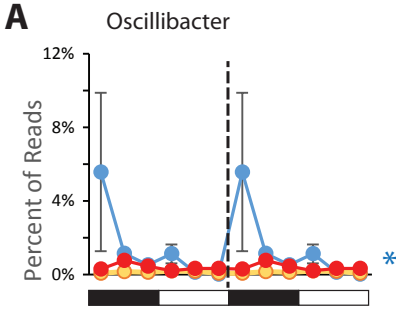


Figure S5

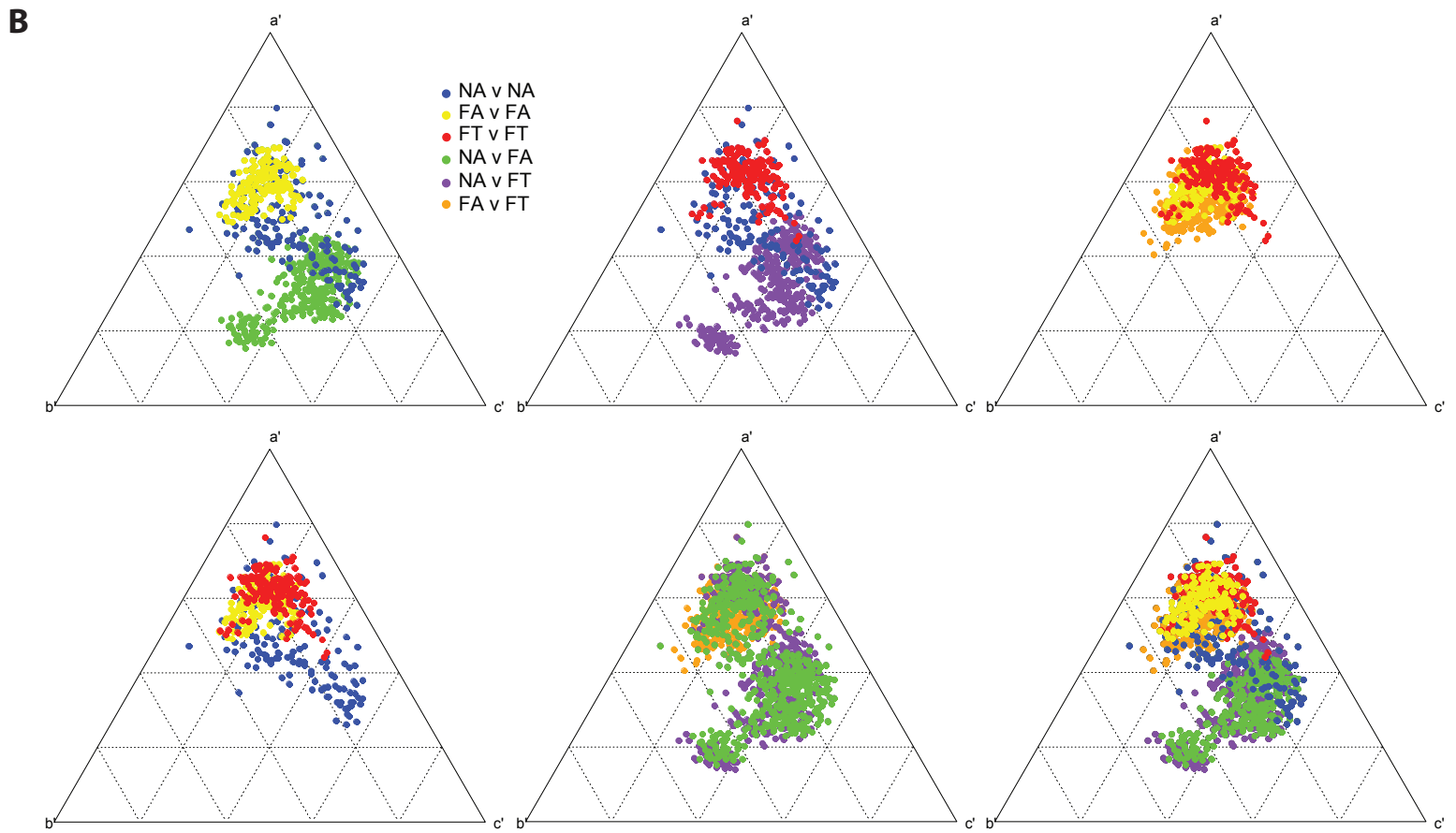
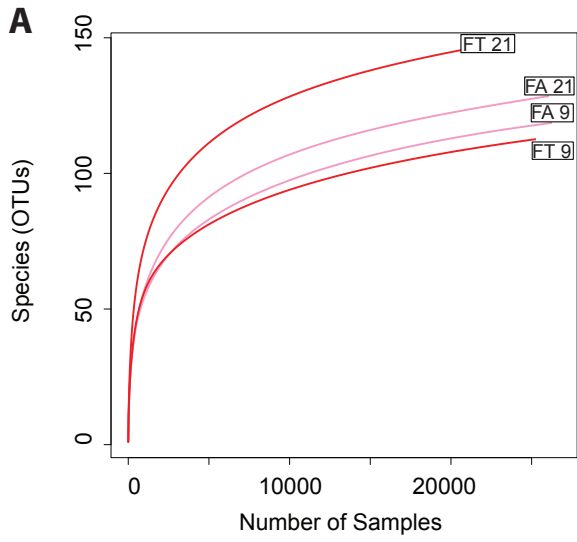


Figure S6

